Article

Improvements in Nanoparticle Tracking Analysis to Measure Particle Aggregation and Mass Distribution: A Case Study on Engineered Nanomaterial Stability in Incineration Landfill Leachates

Kamyar Mehrabi, Bernd Nowack, Yadira Arroyo Rojas Dasilva, and Denise M. Mitrano

Just Accepted

ACS Publications

1 **Improvements in Nanoparticle Tracking Analysis to Measure**
2 **Particle Aggregation and Mass Distribution: A Case Study on**
3 **Engineered Nanomaterial Stability in Incineration Landfill**
4 **Leachates**

5 Kamyar Mehrabi[1], Bernd Nowack[1], Yadira Arroyo Rojas Dasilva[2], Denise M. Mitrano*[1,3]

    1. Empa, Swiss Federal Laboratories for Materials Science and Technology, Technology and Society
        Laboratory, Lerchenfeldstrasse 5, 9014 St. Gallen, Switzerland
    2. Empa, Swiss Federal Laboratories for Materials Science and Technology, Electron Microscopy Center,
        Ueberlandstrasse 129, 8600 Dübendorf, Switzerland
    3. Eawag, Swiss Federal Institute of Aquatic Science and Technology, Process Engineering,
        Ueberlandstrasse 133, 8600 Dübendorf, Switzerland

15 *Submission to Environmental Science and Technology*

22 **Corresponding Author:**
23 Dr. Denise M. Mitrano
24 Eawag – Swiss Federal Institute of Aquatic Science and Technology
25 Process Engineering
26 Überlandstrasse 133
27 8600 Dübendorf
28 Switzerland
29 Phone: +41 58 765 54 91
30 Denise.mitrano@eawag.ch

Abstract

Numerous nanometrology techniques have been developed in recent years to determine the size, concentration and a number of other characteristics of engineered nanomaterials (ENM) in environmental matrices. Among the many available techniques, Nanoparticle Tracking Analysis (NTA) can measure individual particles to create a size distribution and measure the particle number. Therefore, we explore the possibility to use these data to calculate the particle mass distribution. Additionally, we further developed the NTA methodology to explore its suitability for analysis of ENM in complex matrices by measuring ENM agglomeration and sedimentation in municipal solid waste incineration landfill leachates over time. 100 nm Au ENM were spiked into DI H_2O, synthetic and natural leachates. We present the possibility of measuring ENM in the presence of natural particles based on differences in particle refractivity indices, delineate the necessity of creating a calibration curve to adjust the given NTA particle number concentration and determined the instruments linear range under different conditions. By measuring the particle size and the particle number distribution, we were able to calculate the ENM mass remaining in suspension. By combining these metrics together with TEM analyses, we could assess the extent of both homo- and heteroagglomeration as well as particle sedimentation. Reporting both size and mass based metrics is common in atmospheric particle measurements but now the NTA can give us the possibility to apply the same approach also to aqueous samples.

68   **1. Introduction**

69   Qualitative and quantitative identification of engineered nanomaterials (ENM) is complex, as these materials have

70   very low mass, can be highly dynamic in terms of particle agglomeration and reactivity, co-exist with ambient

71   particles in the same size range (i.e. natural analogs) and also often coincide with molecules or macro sized

72   counterparts of the same chemical composition.[1,2] Due to these difficulties, there are limited options to measure

73   ENM size dispersions in natural samples. One of the most promising and prominent solutions which allows the user

74   to measure individual particles at very low (ppt) concentrations in complex samples is spICP-MS. In recent years

75   this technique has received wide spread attention for researchers studying ENM from environmental samples,

76   biological samples, and ENM release from products.[3,4] However, better understanding particle agglomeration

77   dynamics using this technique is in its infancy.[5,6] Transmission electron microscopy (TEM) is another popular

78   option to visualize particle size distribution and agglomeration with particles, even in complex media, but without

79   being quantitative, the technique offers little in terms of being able to robustly characterize the ENM in a system of

80   interest, though validation methods for quantifying particle number have been investigated.[7] Field flow

81   fractionation, while requiring extensive method development, is another analytical option for researchers studying

82   ENM in natural systems.[8-10] While not measuring particles on an individual basis like the previously mentioned

83   techniques, the ability to provide an initial particle size distribution, ENM agglomeration and/or complexation to

84   natural materials is possible. Conversely, some commonly used techniques, such as dynamic light scattering (DLS),

85   can provide misleading results since the average particle size can easily be skewed by a few large particles in a

86   mixtures compared to many small particles.[11] In addition to this, the technique is not material specific and therefore

87   cannot differentiate between natural particles in solution or agglomerates of natural and engineered particles.

88   The NanoSight (i.e. nanoparticle tracking analysis, NTA) offers advantages to measuring ENM in complex systems

89   for its ease of use and unique measurement capabilities. The instrument differs from other light scattering techniques

90   (e.g. DLS) in that it can measure individual particles (opposed to the entire particle population) and that an image of

91   the particles' scattering (although not the particle itself) is recorded.[12] Since the optical configuration employed in

92   NTA analysis allows NM to be simultaneously tracked and analyzed on an individual basis, the resulting data is not

93   an intensity weighted mean but rather a high resolution particle size distribution analysis. Additionally, different

94   materials can be distinguished through their different refractive indices and, importantly, particle concentrations can

95   be measured.[13] These aspects of measurement offer a few advantages; 1) the particle size distribution will not be

96   dominated by the larger, more intensely scattering particles as with DLS, 2) estimating the concentration of particles

97   is possible based on the number of individual particles tracked and extrapolating from the assumed scattering

98   volume calculated from the dimensions of the field of view and the depth of the instruments laser beam and 3)

99   particles with varying light scattering potential can be measured separately by adjusting the camera focusing metrics

100   (e.g. aperture, shutter, brightness, gain etc.) accordingly and analyzing the same sample over multiple runs. Each of

101   these points are advantageous for researchers studying ENM in natural systems, where the aqueous suspensions are

102   often complex and understanding changes in particle size and mass are important characteristics to measure. Until

103   now, extensive method development to better understand a number of these features specifically in particle and

104   mineral rich media has not been exploited, and so while it offers many promising features, the protocols remain to

105   be fully validated. However, the technique does not provide details of particle morphology and there have been

106   limited instances where the technique has been used in complex, natural systems. Some examples of where NTA

107   was implemented in more complex matrices include the study of fullerines in river water,[14] SiO_2 nanoparticles in

108   biological serum,[15] and Gallego-Urrea et al. reviewed the applicability of particle-tracking analysis for the suitability

109   of nanoparticles in a range of matrices including environmental, biological and food samples.[16]

110   To test the applicability of using the NTA to study the stability of ENM in natural environments, Au ENM (used as

111   tracers) were studied to estimate the agglomeration potential of ENM in incineration landfill leachates. Landfills

112   were identified to be one of the predominant compartments that accounts for the final fate of ENM at the end of life

113   stage by material flow modeling and life cycle releases.[17-21] In the current models, landfills are considered to be final

114   sinks because almost no information on the behavior of nanomaterials in landfills is available.

115   Natural colloids are a ubiquitous component of natural water systems and are likely to affect the fate of NM, namely

116   by heteroagglomeration and subsequent settling. In most studies investigating the effect(s) of colloids on ENM

117   stability, ENM interaction with natural organic matter (NOM) has been the most intensely studied even though this

118   fraction of natural colloids is relatively small compared with inorganic solids and larger biopolymers (e.g.

119   biomass).[22-24] In a recent study by Mitrano et. al, the authors investigated the mobility of natural (nano)particles

120   from landfills for municipal solid waste incineration (MSWI) residues and concluded that understanding the

121   geochemical weathering of the landfill slag was essential in relating the type, extent and timing of particulate release

122   from the landfill.[25] Therefore, landfill leachate can be considered a potential source to transport both colloidal and

123   nanoparticulate matter into the environment when they are emitted from landfill leachate.

124   The overall goals of the study were twofold; firstly to improve particle quantification using the NTA to study ENM

125   behavior in complex matrices and secondly to suggest ENM stability in landfill leachates from landfills containing

126   MSWI residues. In terms of method development, we investigated the effects of solution chemistry on measuring

127   particle size and particle number as well as the linear range of instrument detection in these solutions. Additionally,

128   we transformed the NTA raw output (in terms of size and particle number) to mass of analyte to better study the

129   agglomeration of particles over time. The stability of ENM that are deposited into landfills can be analyzed for their

130   agglomeration potential, which in part can help to determine if the particles are likely to remain in the landfill

131   through agglomeration and deposition or be emitted with the leachate as freely dispersed particles. This stability

132   analysis was conducted with pristine Au ENM suspended in synthetic and natural landfill leachate solutions to help

133   elucidate the influence of ionic composition and presence of NOM. Three types of solutions were analyzed

134   including 1) DI water as a control, 2) leachate collected from a landfill for MSWI residues and 3) "synthetic

135   leachate" made from only the major ions as measured in the natural leachate sample. The purpose of creating the

136   synthetic leachate was to measure the effect of major ions on the stability of the ENM without the presence of NOM

137   or other suspended solids found in the natural leachate sample. We then studied the stability of the particles

138   suspended in this solution over time by following changes in particle size (distribution) and mass of analyte

139   associated with each size category using the NTA instrument as well as visually identifying ENM aggregates and

140   complexes using transmission electron microscopy (TEM).

141

2. Materials and Methods

2.1 Standards and Nanomaterials

18 M-ohm DI water was used throughout the study for ENM spiked into water and for making up the synthetic leachate solution. 100 nm citrate stabilized metallic Au (Nanocomposix) were used for calibration and in all experiments in this study. Size distributions corresponded well to TEM analysis provided by the manufacturer and NTA measurements completed in house, with average particle size being measured as 103 ± 11 nm and 103.9 ± 0.6 nm for each measurement, respectively (Figure S1). The hydrodynamic diameter, as measured by DLS, was 124.7 ± 5.6 nm and the zeta potential was -26.mV. The Au concentration of the stock solution was given by the manufacturer but was verified via total Au analysis (ICP-MS). Given the solution concentration and particle size, we could therefore calculate the total particle number concentration in the stock solutions and make appropriate dilutions (e.g. for the calibration curve) based on this information.

2.2 Water Quality Analysis: Natural and Laboratory Prepared Leachate Samples

A subset of the same MSWI leachate samples used in Mitrano et. al. were also used for this current study.[25] Landfill samples were taken from the ZAB Deponie, located in Flawil, Switzerland. In this landfill, MSWI residues (slag from both the bottom ash and fly ash) as well as wastewater incineration residues (sludge incineration) are collected. The leachate samples were taken directly from the main outflow into the settling basin (hereafter labeled "natural leachate"). Natural leachate samples were filtered through a 0.45 µm filter (Whatman; cellulose nitrate membrane) before spiking ENM for stability studies to remove particles too large to be measured by the NTA and that would potentially obscure ENM observation.

The pH of the natural leachate was measured by a Metrohm 827 pH meter and found to be 7.8 +/- 0.3. Samples were prepared for dissolved organic carbon (DOC) analysis with filtration through a 0.45 µm filter (Whatman; cellulose nitrate membrane) into glass bottles and analyzed by a commercial laboratory (Bachema AG). An initial survey of water chemistry parameters of the leachate filtered through a 0.45 µm filter was conducted to determine which ions were present in significant concentrations by IC analysis for anions (F^-, Cl^-, NO_2^{2-}, Br^-, NO_3^-, PO_4^{3-} and SO_4^{2-}) and ICP-OES analysis for cations (Na^+, K^+, Mg^{2+} and Ca^{2+}). Bachema AG measured the final selection of major ions that were identified as significant contributors to the solution chemistry with IC measurements (Cl^- and SO_4^{2-}) and ICP-OES analysis (Na^+, Ca^{2+}). We derived a simulated leachate to examine the stability of nanoparticles consisting of the major ions existing in the natural leachate sample (e.g. Na^+, Ca^{2+}, Cl^- and SO_4^{2-}). We collected the landfill leachate on three separate occasions, in order to work with "fresh" leachate so we could be assured that the particulate composition, pH, etc. was as accurate as possible without sedimentation as we were working on the method development. The freshest (third) of these samples was used as the natural leachate sample in this study, where the final results were collected together over a short time span, but the synthetic leachate composition was derived from the first sampling time point at landfill when all of the water chemistry parameters were measured, hence the small differences between the total salts between the "natural" and "synthetic" leachate solutions. However, the overall

177   magnitude of all the components was similar between to the two leachates used in this study. See Table S1 for water

178   chemistry of natural and synthetic leachates.

179

180   *2.3 NanoSight (NTA) Analysis*

181   NTA measurements were performed with a NanoSight NS500 (NanoSight, Amesbury, United Kingdom). The

182   samples were injected in the sample chamber with sterile syringes by means of syringe pump with a constant rate of

183   injection. All measurements were performed at room temperature. 100 nm Au nanoparticles were analyzed first in

184   DI water and then in the leachates. The software used for capturing and analyzing the data was NTA 3.0. Triplicate

185   samples were measured for 4 min, with average valid particle tracks ranging from 50 to 5000 for each analysis. The

186   camera level was set to 1 for every measurement to ensure standardized analysis and to eliminate possible bias

187   induced by further adjusting parameters for each sample, but the camera focus was adjusted daily depending on the

188   sample. The camera level determines the brightness of the image and thus partially is responsible for the particles

189   that are selected to be tracked by the NTA. The levels use preset combinations of shutter and gain. For high

190   sensitivity camera systems, the camera levels also incorporate appropriate thresholding pixel levels to improve

191   image contrast. With these conditions, that were made constant throughout our analysis, we visually noted the same

192   brightness of the ENM in solution across experimental sets and did not observe any additional (i.e. natural) particles

193   during any of the measurements.

194   Each influx of sample and video produced a histogram depicting particle size and concentration. The information

195   regarding individual particles were exported to an excel sheet for further data processing, but the concentration

196   reported by the NTA was taken directly without any additional adjustment. Additionally, we calculated the total

197   mass of analyte (particles) in each video distributing the total particle number proportionally over the particle size

198   distribution histogram. In this way, we could determine if a mass balance was kept constant over the analysis time.

199   Given these test conditions, we could determine if the total analyzed concentration was decreasing and particles

200   were not being measured (e.g. from sedimentation) or simply if the NTA was recording fewer, larger particles.

201

202   *2.4 Calibration of the NanoSight (NTA)*

203   The calibration of the NTA was conducted for two main reasons; 1) to define the linear range in terms of particle

204   concentration and 2) to determine if the solution chemistry (or matrix) had an influence on the particle number

205   measured at various concentrations. To achieve these goals, the three different experimental solutions (DI H_2O,

206   synthetic leachate and natural leachate) were spiked with Au ENM in five particle concentrations including: a blank

207   (i.e. no added ENM), 0.25×10^8 particles/mL, 0.5×10^8 particles/mL, 1×10^8 particles/mL and 1.5×10^8

208   particles/mL. In terms of mass based concentration, for 100 nm particles this equates to approximately $150 - 800$

209   μg/L. These concentrations were based on diluting the stock Au ENM solution (particle concentration and size given

210   by the manufacturer and determined in house, see section 2.1) into the appropriate matrix. The samples were

211   prepared in triplicate and analyzed directly after preparation. Two metrics were considered in this analysis, particle

212   size (distribution) and measured concentration. Particle size evaluations were performed to ensure that the

213   instrument was capable of successfully identifying the pristine particle size in various solution chemistries and that

214   no agglomeration of the ENM was occurring over a very short period of time (i.e. T=0 hr measurements). The

215   concentration measured by the NTA instrument could be compared to the expected (spiked) concentration into each

216   solution, where any deviation from the 1:1 spiked particle number to measured particle number ratio would indicate

217   an adjustment would need to be made to correct the concentration of particles measured by the NTA.

218

219   *2.5 Stability of ENM in MSWI Landfill Leachates*

220   Stability tests were conducted at 0.5×10^8 Au particles/mL, as this was determined to be within the appropriate

221   linear range of particle concentrations for the NTA under our test conditions. For each of the three water chemistries

222   investigated, triplicate samples were prepared and analyzed over a series of time points up to 24 hours. At time zero,

223   samples were spiked with the appropriate amount of Au particles into a 50 mL polypropylene vial containing the

224   solution of interest and shaken end-over-end by hand for 30 seconds. Using a polypropylene syringe, an aliquot of

225   the sample was then taken 1 cm below the surface of the water/air interface and analyzed by NTA as described in

226   Section 2.3. The vials then remained standing upright and still for all subsequent time points being sampled in the

227   same manner for NTA analysis for each time point. This method allowed us to investigate three metrics: 1) particle

228   size (change) over time, 2) particle number remaining in solution over time and 3) particle or particle agglomerate

229   settling over time. The first metric was determined directly by the NTA and therefore we have simply re-plotted the

230   size output reported from the instrument for this metric. Particle concentration was also directly measured by the

231   NTA but this data is reported both as the raw output and as adjusted by the calculated calibration curve to correct for

232   particle number measurement differences in varying solution chemistries; described in more detail in Section 2.6.

233

234

235

236   *2.6 NanoSight (NTA) Data Evaluation*

237   Individual valid track measurements (i.e. particle measurements) were exported directly from the NTA software into

238   excel via a .csv data file. These individual particle measurements were then plotted into a histogram in excel. The

239   particle number was measured directly by the NTA software and the number was taken directly from the report

240   generated by the NTA without any adjustment. This particle measurement data was also used to generate the

241   calibration curve for Au ENM suspended in the various waters at different known particle concentrations. The slope

242   of each calibration curve was used as a "scaling factor" to adjust the particle number concentration and/or mass

243   concentration appropriately in experimental sets. The raw number concentration and the mass concentration was

244   multiplied by the scaling factor to adjust for instrumental differences of particles in different matrices. To calculate

245   the mass concentration from the particle number distribution, the following steps were taken (see Equation 1): 1)

246   make the particle size distribution histogram based on the NTA output, 2) proportionally distribute the total particle

247   number across the particle size distribution histogram to have the number of particles in a given size range

248   (histogram bin size, 2 nm), 3) multiply the number concentration in each bin by the associated particle diameter and

249   transform the diameter metric into a volume metric, 4) sum all mass calculations from all bins in the histogram and

250   finally 5) multiply by the elemental mass (in this case, Au).

$$m = \rho \sum_{i=1}^{n} \left(\overline{V}_{c,i} \frac{1}{6} \pi d_i^3 \right)$$

251
252   **Equation 1:** Calculations for converting the particle size distribution histogram and particle number generated from
253   the NTA into mass of analyte measured. The diameter of particles in a particular bin i (d_i) is multiplied by the
254   number concentration of gold particles in a particular bin ($V_{c,i}$) and transformed from diameter to volume. This value
255   is then summed for all bins in the histogram and multiplied by the particle density (ρ) to determine the total mass
256   of analyte in the system.
257

258   *2.7 Transmission Electron Microscopy (TEM)*

259   Pristine 100 nm Au nanoparticles were spiked at the same concentration as in the NanoSight analysis (i.e.

260   approximately 1 mg/L or 0.5 x 10^8 particles/mL for 100 nm Au ENM) into each of the leachate samples. Grids were

261   prepared for the DI H_2O, synthetic and natural leachate samples at T = 0 hr and T = 4 hr. At each time point, sample

262   vials were vigorously shaken and 3 mL of the sample was transferred to a polypropylene vial where particles were

263   deposited directly onto TEM grids by centrifugation using a swinging bucket rotor, with rotation speed of 45000

264   rpm for 1 h; conditions which completely deposited all particles > 10 nm in size onto the carbon-coated Cu TEM

265   grid. Samples were gently washed to remove residual salt by moving the grid through a drop of MilliQ water on a

266   piece of parafilm 3 – 5 times. The centrifugation TEM grid preparation alleviates many artifacts that disrupt typical

267   drop deposition TEM grid preparation. Therefore, this method gives us additional confidence that we can identify

268   agglomeration of particles in the native solution opposed to any drying effects from traditional drop deposition TEM

269   grid preparation.

270   Particle images were obtained via scanning transmission electron microscopy (STEM) using a JOEL 2200FS

271   TEM/STEM operated at 200 kV. The nominal spot size of the STEM probe was 0.7 nm using a beam convergence

272   angle of 10.8 mrad. High-angle annular dark field STEM micrographs were recorded using an inner detector angle

273   of 100 mrad, while the bright-field STEM images were recorded with a detector angle of 15 mrad.

274

275   **3. Results**
276   *3.1 Measurement of ENM in the presence of natural particles*

277   The NTA camera settings can be set to measure particles with a lower refractivity, such as the natural particles

278   present in landfill leachate, as shown in our previous work[25] and in Figure 1, panel A. In this case, the leachate was

279   filtered through a 0.45 µm filter and particles are visible in the solution up to that size cut off. When the settings are

280   adjusted to those that can properly measure Au ENM (i.e. a lower camera level to capture only the brightest

281   particles), no natural particles were observed in the same natural leachate sample when leachate samples captured at

282   low camera level with no spiked Au ENM (Figure 1 B, red trace). However, when Au ENM are spiked into the

283   solution, a similar distribution is observed for the main particle size distribution in both DI H_2O and the landfill

284   leachate (yellow and green traces, respectively), indicating that the additional natural particles do not disrupt the

285   direct measurement of ENM due to the change in matrix. Neither do we observe additional particles in the Au ENM

286   particle distribution when the particles are spiked into the natural leachate compared to DI H_2O. In the case of the

287   Au ENM spiked into the leachate, there are only some slightly larger particles observed due to Au ENM

288   homoagglomeration between spiking the solution and analysis. This exercise confirms our ability to detect Au ENM

289   in the presence of natural particles in our test matrices.

290   In all blank samples (i.e. those that did not contain any added Au ENM), including the natural leachate, the number

291   of observed particles under typical nanoparticle analysis conditions was close to zero or zero. This indicates that our

292   method to observe only the ENM while avoiding measurement of the natural particles in solution with a lower

293   refractivity index was successful and therefore we do not measure a significant number of false positives (i.e. natural

294   particles appearing as ENM in the results).
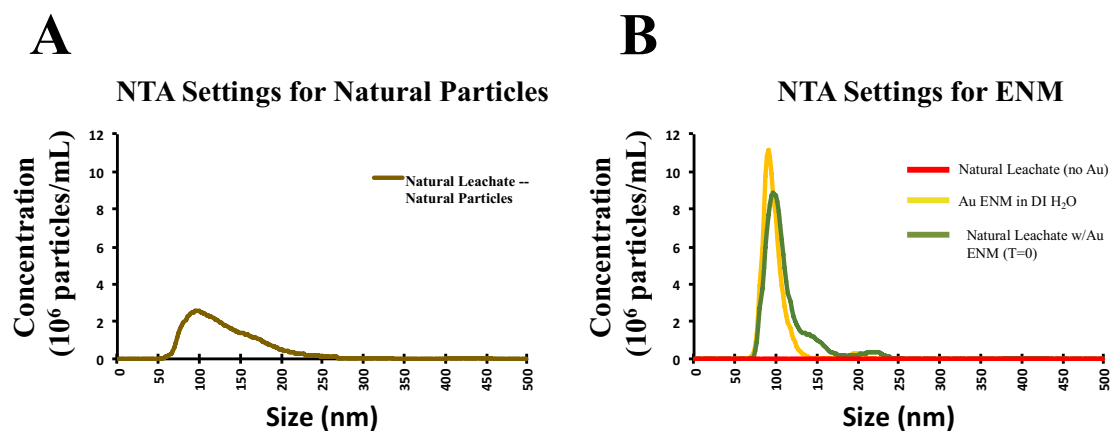
295

296   **Figure 1:** (A) NTA set to measurement conditions optimal to measure natural particles in solution, as in the
297   natural landfill leachate from MSWI residues, filtered through a 0.45 μm filter. (B) NTA camera level set to a
298   lower level intend to measure bright particles (i.e. those with a high refractivity index) but still measuring the
299   same leachate as panel A. Natural leachate with only natural particles (red trace), Au ENM spiked into DI H_2O
300   (yellow trace) and Au ENM spiked into natural leachate (green trace) are shown together. Here it is seen that
301   natural particles in the landfill leachate are only visible on the higher camera level in Panel A, but not when
302   the camera level is adjusted lower in panel B (red trace). However, spiked Au ENM are clearly detected in
303   both DI H_2O and the natural leachate with no interference (e.g. additional background) from the natural
304   particles in the leachate.

305

306   *3.2 Calibration of ENM Concentration for the NTA*

307   The NTA calibration of ENM concentration served two purposes; 1) to determine the linear range between

308   measured and expected concentrations of ENM in different solution compositions and 2) to identify the scaling

309   factor of this relationship when it deviated from the expected 1:1 ratio of added particle number to measured particle

310   number. The particle number was taken as given by the NTA 3.0 software. As shown in Figure 2A, a liner

311   relationship is exhibited for all sample solutions with a particle concentration below 1×10^8 particles/mL and the

312   standard deviation between triplicate measurements was relatively small. Measured particle concentrations deviated

313   from the linear calibration line above 1×10^8 particles/mL.

314   Despite defining a linear range for particle number concentrations in each of the solutions, in every instance there

315   was a higher measured particle concentration compared to the known particle concentration. Therefore, in every

316   case the steeper slope exhibited by the calibration line represents an overestimation in particle number concentration

317   and therefore the particle number measured by the NTA in the experimental samples had to be appropriately scaled

318   to derive the correct particle number in solution by using the slope of the linear portion of the calibration curve. This

319   scaling factor was different for each of the three solutions measured. The exaggeration in particle number was

320   highest for the DI H$_2$O samples (up to a factor of three) but leachate samples were also overestimated by

321   approximately a factor of two. A similar particle number concentration was observed in both the synthetic and

322   natural leachate samples. Overall, this indicates that the matrix can play a large role in how the NTA software

323   ultimately calculates particle number and so a calibration curve should be made for each new solution of interest to

324   derive the correct scaling factor during experimental tests.

325   *3.3 NTA Analysis of ENM Particle Stability in Incineration Waste Landfill Leachate*

326   ENM stability experiments were conducted with a particle concentration of 0.5 x 10^8 particles/mL since this was

327   within the liner range identified by the calibration for all solutions of interest. The particle size distribution at each

328   dilution point and in every water chemistry was consistent and with relatively good agreement to the average

329   primary particle size (Figure 2 B-D). The NTA did appear to slightly overestimate the number of larger sized

330   particles in the distribution (as evidenced by the longer whiskers for the larger particle diameters in Figure 2 B-D)

331   even though the distribution was more Gaussian when measured by TEM (Figure S1). Nevertheless, since the

332   measured particle size was consistent across all dilution factors and across all solutions investigated, the discrepancy

333   in measured versus known particle number cannot simply be due to agglomeration.

334
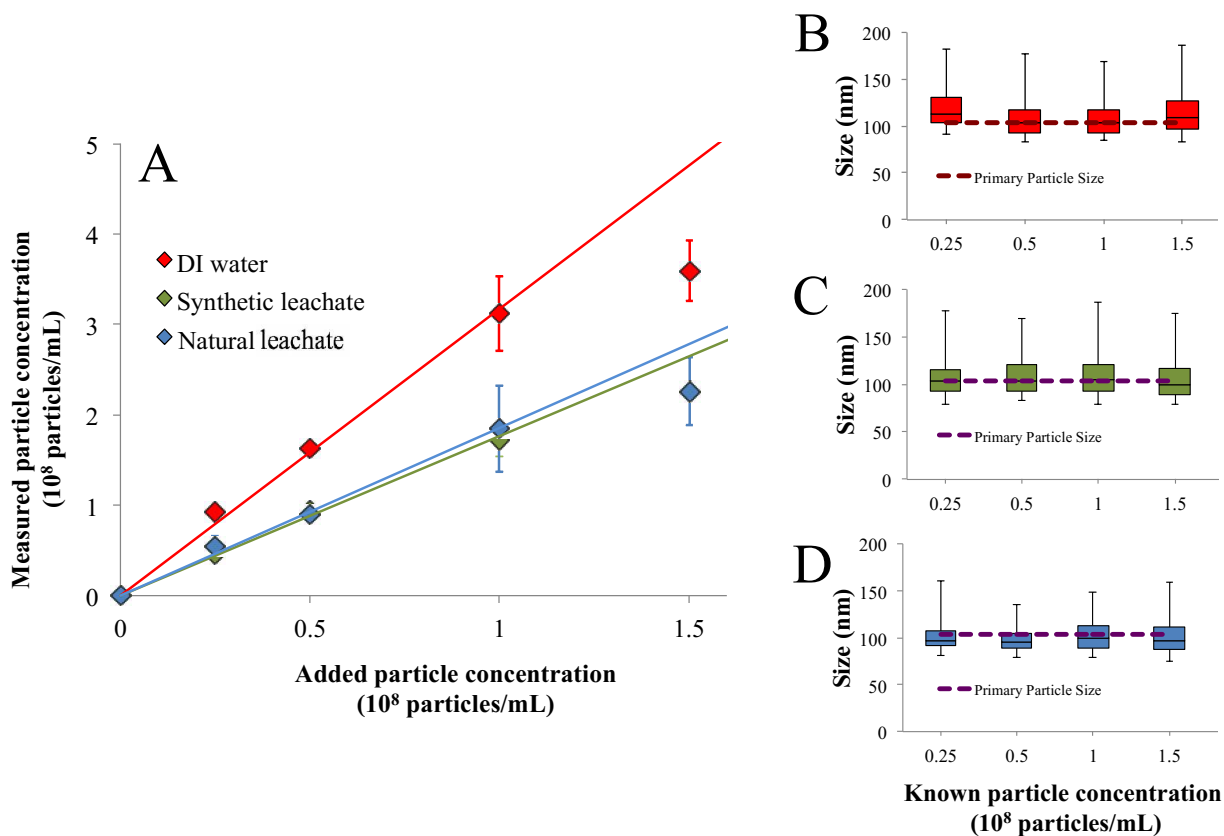
335
336   **Figure 2:** Particle number concentration calibration curves of Au nanoparticles suspended in DI H$_2$0, synthetic and
337   natural MSWI landfill leachates compared to the expected 1:1 know particle number to measured particle number
338   ratio (A). A linear regression line of each of the calibration curves is presented through the linear portion of the data

339 set (0 to 1×10^8 particles/mL) with a predicted extension of the regression line until 1.5×10^8 particles/mL to
340 exemplify how these data are not in the linear range. Particle size distribution of particles measured at different
341 dilutions in DI H_2O (B), synthetic (C) and natural MSWI (D) leachates. For the box plots, 25% quantiles appear
342 within the box plot with average particle size indicated by black line therein. Whiskers represent 95% of particle size
343 distribution (outliers not shown). Purple dashed lines indicate Au ENM primary particle size (100 nm).
344

345 ### 3.3.1   ENM Stability – Average Particle Size and Particle Size Distribution

346 The average particle size in DI H_2O remained constant throughout the entire experimental timeline, up to 24 hr

347 (Figure 3A). This indicates that at this concentration and with no additional salts or particulate matter, the particles

348 are stable in solution for extended periods of time. In synthetic and natural landfill leachates (Figure 3, panels B and

349 C), the average particle size generally increased over the course of the 24 hr experiment.

350 Not only did the average size increase in the leachate samples, but the size distribution became much wider as well,

351 indicating agglomeration of the primary particles over time. Compared to the ENM distribution in DI H_2O, which

352 remains narrow and constant, the particle size distribution for synthetic and natural landfill leachates began to

353 broaden immediately after particle spiking. The relative rate of agglomeration appeared somewhat slower in the

354 synthetic leachate compared to the natural leachate. Differences in solution chemistry, especially differences in

355 DOC and salt concentrations, can contribute to the stability of the particles. In the case of the synthetic leachate,

356 since the solution is made entirely of added salt, homoagglomeration is the only possibility for the measured

357 increase in size. However, in the natural leachate, heteroagglomeration between the Au ENM and natural material is

358 possible. Since under the conditions we are operating the NTA only the ENM are visible, a single ENM or ENM

359 cluster adhered to natural particles will move more slowly (increased particle size equals decreased speed of

360 Brownian motion) and therefore be recorded as a (single) larger particle. Indeed, in the natural leachate sample the

361 average particle size is larger than in the synthetic leachate sample. (see Figure S2 and Table S2).

362
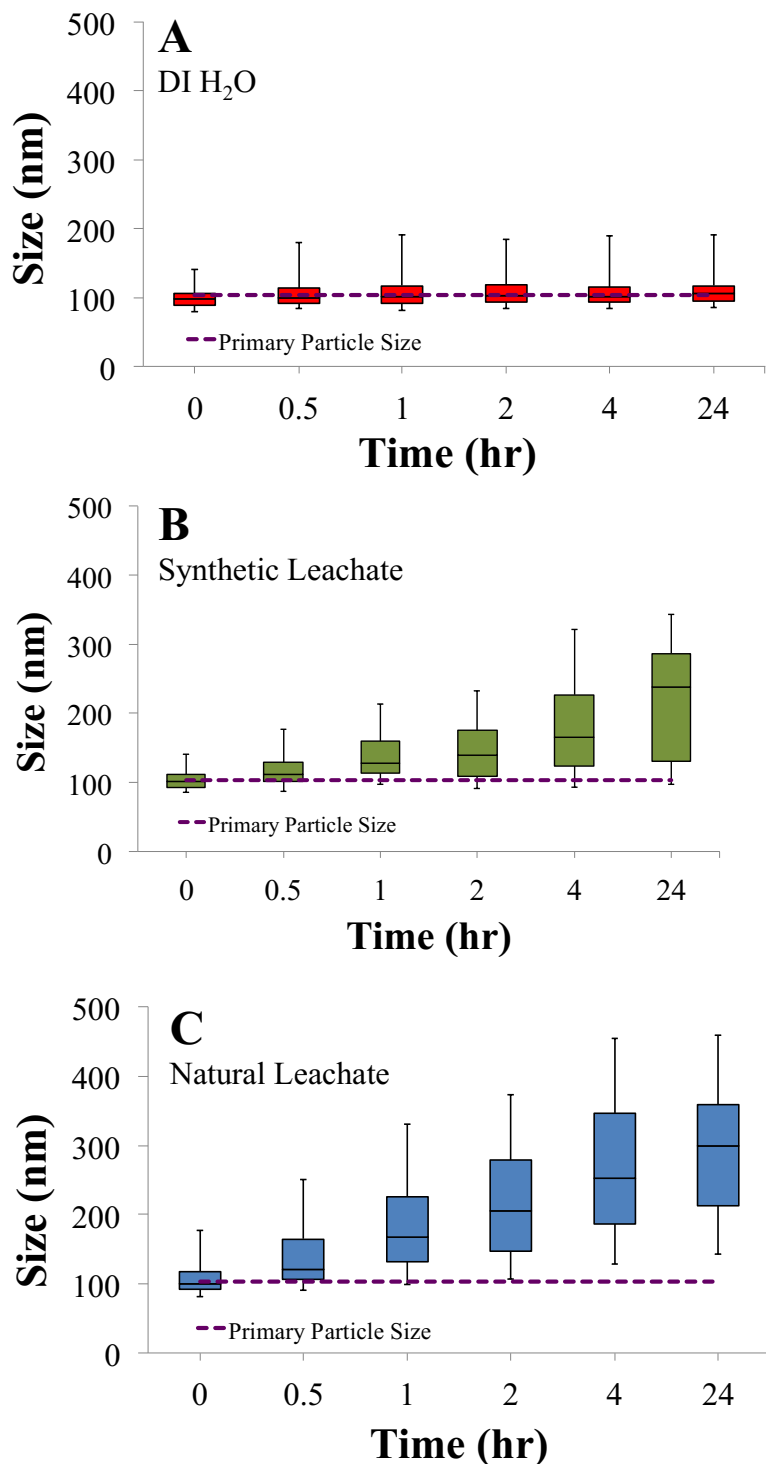
363
364 **Figure 3:** Size distribution of particle (aggregates) over time in A) DI H$_2$O, B) synthetic landfill leachate and C)
365 natural MSWI landfill leachate. 25% quantiles appear within the box plot with average particle size indicated by
366 black line therein. Whiskers represent 95% of particle size distribution (outliers not shown). Purple dashed lines
367 indicate Au ENM primary particle size (100 nm).
368
369
370

371   *3.3.2   ENM Stability – Particle Number*

372   The importance of calibrating the NTA for particle number in various matrices is exemplified when measuring the

373   stability of particles over time by analyzing the change in particle number. For example, when the same

374   concentration of Au ENM is spiked into the leachate solutions, the raw output from the NTA instrument shows a

375   disparity in concentration between the initial particle number concentration in DI H_2O, synthetic leachate and the

376   natural leachate (Figure S3). However, when these particle numbers are corrected based on the scaling factors

377   obtained from the calibration curve, the T = 0 hr concentrations are all very similar between the various solutions

378   (Figure 4), albeit at a lower total particle number measured since in all instances the NTA overestimates the particle

379   number.

380   The particle number concentration in DI H_2O remained constant over time. Along with the particle size remaining

381   unchanged, this further suggests that particles were stable over the 24 hr experiment and the NTA was able to

382   consistently measure them in solution. Synthetic and natural leachates both exhibited decreases in particle number

383   concentration over time. However, in this instance the number concentration given directly by the NTA instrument

384   needed to be corrected by the scaling factors determined by calibrating the instrument to correctly measure the

385   particle number in these various solutions (Figure 4). In the raw results (Figure S3), the number of particles

386   measured in both synthetic and natural leachates appear similar and their decrease over time tracks one another.

387   However, when scaling the particle number appropriately based on the calibration curve, it becomes evident that

388   particles suspended in the synthetic leachate seemingly disappear from solution at a faster rate than those suspended

389   in the natural landfill leachate solution (Figure 4). This increased stability in the natural leachate is somewhat

390   expected because when a solution contains DOC the stability of ENM is often increased.[26] Since the synthetic

391   leachate is comprised only of a salt solution that mimics the composition of the natural leachate, we can suggest that

392   the increased stability of the ENM in the natural leachate is due to the DOC.

393
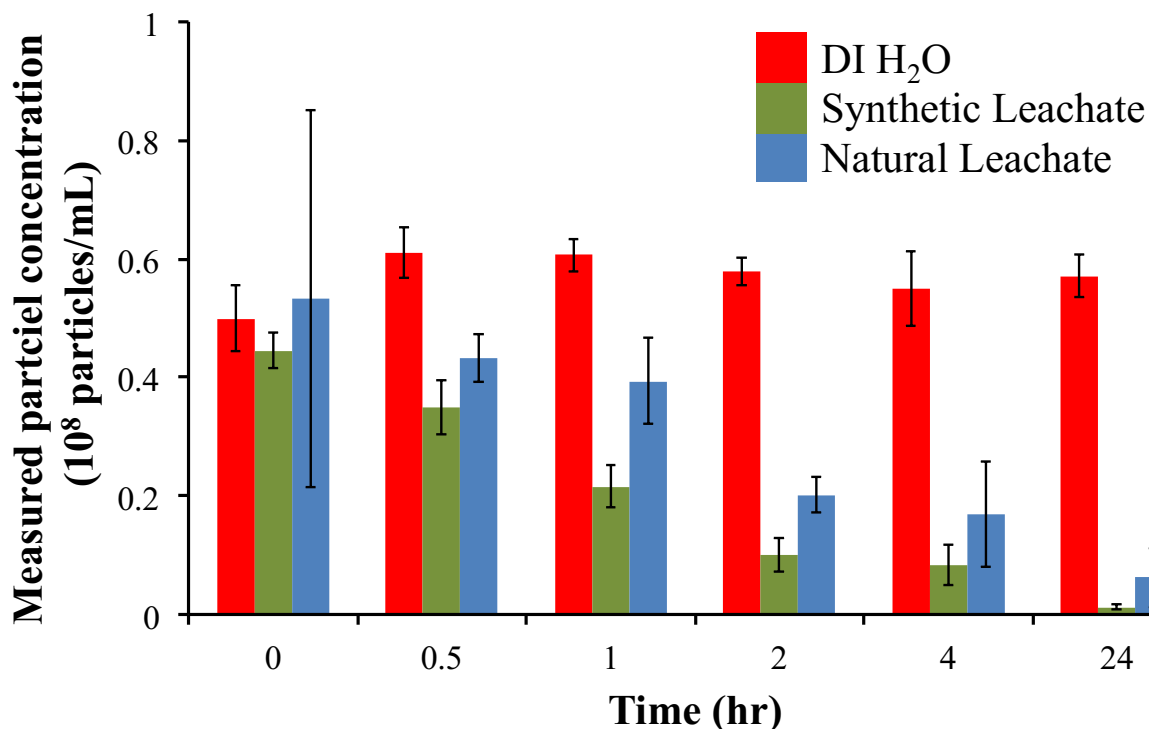
Figure 4: NTA measured particle number concentration of 100 nm Au particles over time in DI H_2O (red bars), synthetic leachate (green bars) and natural MSWI landfill leachate (blue bars). Particle number concentration is based on the calibration curve, it is notable that the particles in the natural leachate samples appear to show an increased stability compared to the synthetic leachate solution, a result that was not visible without the correction factor applied. Error bars indicate results of triplicate experiments.

3.3.3 ENM Stability – Mass Evolution

However, Figure 4 only relays information about particle number but does not take into account the particle size that was measured in each solution (Figure 3). While in many studies the decrease in particle number is taken to imply removal of particles from the leachate solutions (e.g. through settling, etc.), Figure 4 simply shows that there are fewer particles in the leachate solutions. This information can be combined with the particle size distributions (Figure 3) to determine the total mass of Au remaining in the system at any given time point. If, during this analysis, the observed total Au mass in solution decreases then particles are indeed settling from solution. The total mass of the remaining ENM in solution is shown in Figure 5. The initial calculated mass of all samples was similar, at approximately 0.75 mg Au ENM/L. However the stability of ENM exhibited a different behavior over time depending on the solution they were suspended in. The total mass of Au ENMs suspended in DI H_2O and synthetic leachate were relatively stable, with the mass fluctuating less than 25% on average over the course of 24 hrs. However, taken together with the particle size and particle number data (Figures 3 and 4, respectively), different conclusions can be drawn in terms of the particle behavior between these two suspensions. In DI H_2O, there was little change in terms of particle size, particle number and particle mass suggesting that the pristine particles were stable in solution with no agglomeration or settling. In contrast, in synthetic leachate, the particle size increased, the particle number decreased but the mass of particles remained steady. Increasing particle size indicates

417   agglomeration, as does the decrease in particle number since homoagglomeration is the only possibility in this

418   solution. However, because the particle mass remains steady over time, the entire initial mass is accounted for in

419   solution throughout the first 4 hrs of the experiment and so little settling of the agglomerates has occurred. Because

420   the mass decreased by the 24 hr time point, we hypothesize there is more agglomeration and subsequent settling

421   from solution in this sample at extended time points.

422   Just as with the synthetic leachate solution, in the natural leachate preparation particle size was noted to increase

423   over time while particle number decreased. Yet the behavior of Au ENM in the natural leachate is different from its

424   more simplistic counterpart because the total calculated mass seemingly increases up to four times the initial

425   concentration observed in the sample at time zero. While some homoagglomeration is still likely in this sample, we

426   hypothesize that the incorrect overestimation of mass in this instance is due largely to heteroagglomeration. This can

427   be explained by the fact that Au ENM can adhere to other larger natural material (e.g. clays, silicates, DOC, etc.) in

428   the leachates and thus the bright ENM particles observed by the NTA are moving slower than their "free" pristine

429   counterparts. Unlike the synthetic leachate where the total mass remains steady because homoagglomeration is the

430   only option, heteroagglomerates of Au ENM and natural material in the natural leachate is visualized as one, larger

431   (ENM) particle because the NTA is simply tracking the speed of the more reflective ENM adhered to the natural

432   matter. These heteroagglomerates are then sized based on their slower diffusion speed, and thus sized larger, even if

433   the aggregate contains a smaller ENM than the complex that is being tracked by the NTA. Therefore, when

434   calculating the mass from particle size and number, the total mass is significantly overestimated. Furthermore, the

435   high variability between replicates is an indication of ENM agglomeration in the sample.
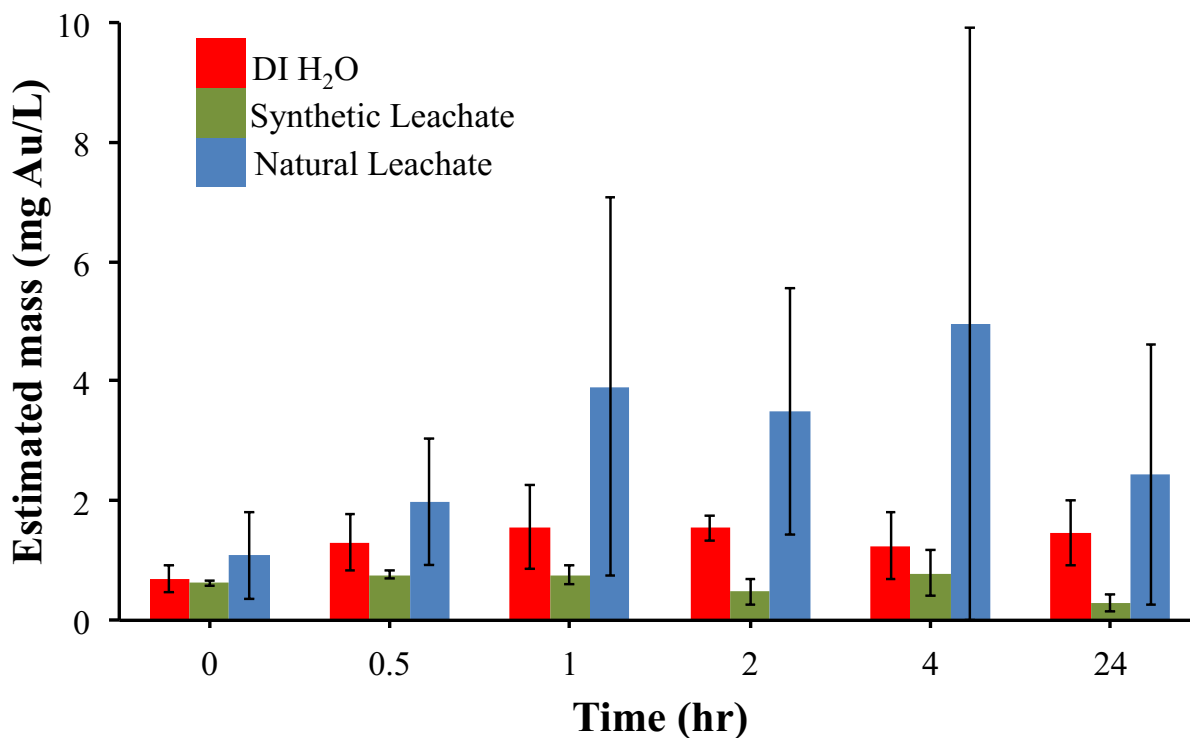
436

437

438

439

440

441
442 **Figure 5:** Calculated mass of Au ENM over time based on NTA measured particle size and (adjusted) particle
443 number concentrations for DI H_2O (red bars), synthetic landfill leachate (green bars) and natural leachate (blue
444 bars). Error bars indicate triplicate experiments.
445

446 *3.4 Visualization of Particle Aggregation with Transmission Electron Microscopy (TEM)*

447 While often morphology and agglomeration is not studied with TEM because with drop deposition there are known
448 artifacts when drying the sample on the grid, the technique used here to centrifuge the suspension so that particles
449 are sedimented onto the grid directly from solution better preserves their natural state and so the extent of
450 agglomeration can be (qualitatively) estimated. One caveat of measuring very heavy elements (i.e. the Au ENM) in
451 the presence of natural particles (i.e the clays, silicates and DOM of the natural leachate) is that it is difficult to
452 image both materials simultaneously due to their different intensities in the image. Therefore in the bright field
453 images presented here the Au ENM appear very dark but any natural material in solution appear much lighter (only
454 applicable in the natural landfill leachate). While this may not be definitive evidence of particle behavior alone,
455 taken together with the results from the NTA experiments a conclusion about agglomeration can begin to be drawn.
456 In all samples, TEM analysis shows that initially Au ENM are dispersed with little or no homoagglomeration or
457 heteroagglomeration in the systems (Figure 6, top row of images). However, after four hours in suspension the
458 behavior and stability of the spiked ENM begin to diverge. In the DI H_2O sample, it appears particles continue to be
459 well dispersed as single particles. This is also what was expected given that both the particle size and particle
460 number was measured as constant over four hours by the NTA (Figure 3, panel A and Figure 4, panel B). In the

461   synthetic leachate sample, additional homoagglomerates of Au ENM are seen and finally in the natural leachate we

462   can see aggregates associated with natural (light colored) material.

463
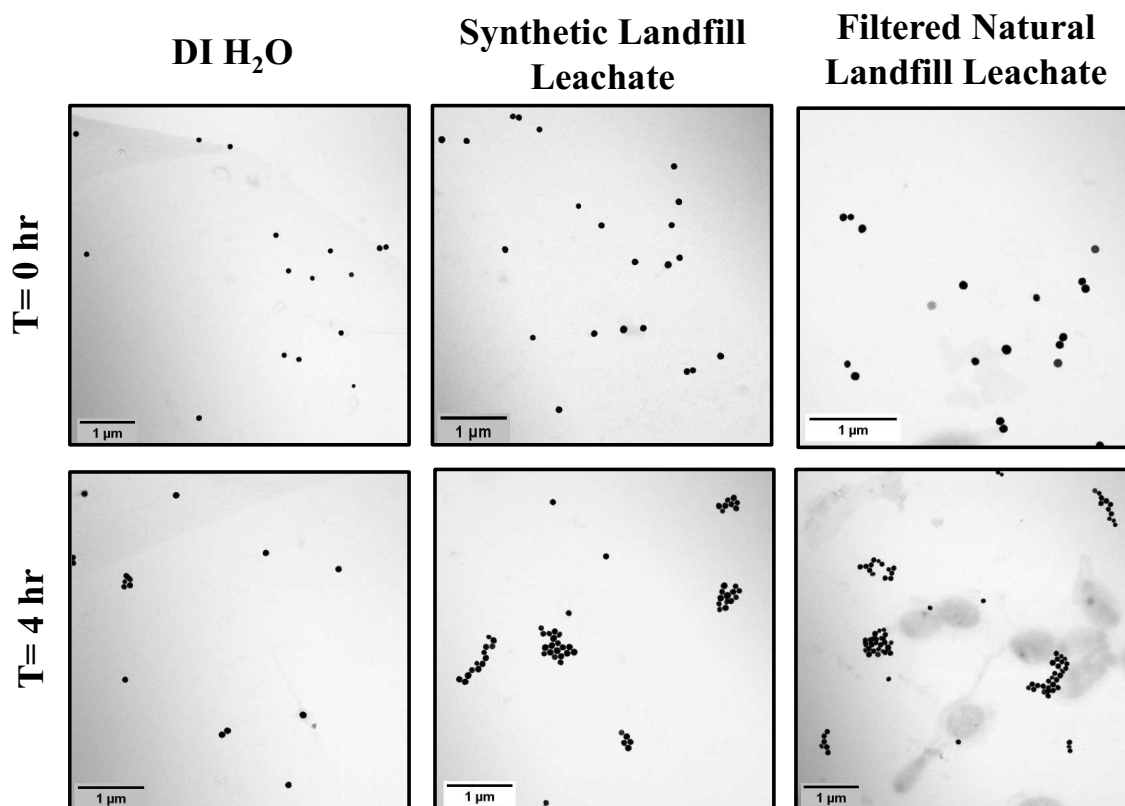
464
465   **Figure 6:** TEM images of Au ENM agglomeration state at T =0 hr and T=4 hr in DI H$_2$O, synthetic landfill leachate
466   and natural landfill leachate (filtered through 0.45 □m filter). Disperse, single particles are evident in all T= 0
467   samples and the DI H$_2$O sample after 4 hrs, yet agglomeration is noted in both synthetic and natural landfill
468   leachates after 4 hrs in solution. In the case of synthetic leachate, homoagglomeration (rather than
469   heteroagglomeration) is evident; likely due to the high concentration of ENM dispersed in a solution with a
470   relatively high salt concentration. In contrast, the ENM suspended in the natural leachate sample seemingly are
471   affected by homoagglomeration as well as heteroagglomeration to the natural particles in the leachate.
472

473   *4. Discussion*

474   *4.1 Suitability and advantages of NTA to measure ENM in complex systems*

475   The suitability and advantages of using the NTA to measure ENM in complex systems was examined in our case

476   study investigating the stability of ENM in landfill leachates. The feature of discerning intensely scattering ENM in

477   a solution of incidental particles has not yet been fully exploited but is of particular relevance in environmental

478   ENM research. Many common and relevant ENM (e.g. Ag and Au particles) have a higher refractivity index than

479   their natural colloidal counterparts (such as clays, silicates, etc.) and the camera settings can be adjusted to "blind"

480   out the natural background and only track the brighter, engineered particles in solution. The relative refractive index

481   of particles in these solutions is very important for the measurement and analysis of the ENM considering the

482   multitude of natural particles existing in solution. In this way, we can easily detect the ENM above the natural

483   background of incidental particles with lower refractivity index in the solution. van der Pol et al. validated a protocol

484   to determine the refractive index of nanoparticles in suspension using NTA, specifically highlighting the usefulness

485   of exploiting this difference in biological and clinical samples.[27] While the sensitivity of the method in terms of

486   observing particles in increasingly complex media may vary depending on the test media, by making a calibration

487   curve of known particles in the media of interest should allow one to determine the ability to measure spiked

488   particles above a natural background with varying mineral and organic contents.

489   With the use of NTA, precise details of ENM stability can be investigated by obtaining multiple metrics including

490   ENM (agglomerate) size, particle number in solution and, ultimately, relating this to the calculated mass of analyte

491   in solution. By selecting different water chemistry variables and measuring over time, we could better monitor these

492   trends and test the applicability of NTA to measure ENM stability in landfill leachates. In DI H_2O we found that

493   particle size, particle number and analyte mass remained constant over time. This solution therefore gave us a

494   benefit in terms of understanding NTA analysis for "baseline" conditions. This evaluation of these reference

495   conditions could then be compared to the results obtained when suspending ENM in assorted leachate chemistries

496   that may induce additional particle (in)stability. Of the two experimental solutions, the synthetic leachate solution

497   had only soluble components (i.e. ions) and pH affecting ENM stability. From the size increase, particle number

498   decrease but overall conservation of mass in solution, we determined that the primary particles were

499   homoagglomerating but were otherwise stable in solution. While the result of ENM homoagglomeration in a salt

500   solution itself is not novel, the measurement techniques and metrics obtained to come to that conclusion are. Using

501   the natural leachate, after 0.45 µm filtration, included the additional complexity of other particulate matter and DOC

502   in the solution chemistry. It has been suggested that homoagglomeration of ENM is not as likely as

503   heteroagglomeration between ENM and natural particles in environmental systems. In this case, we observe both

504   homo- and heteroagglomeration but it is likely that the homoagglomeration is mainly due to the high Au ENM

505   concentration needed for NTA detection and this is less likely to occur in a real environmental sample where the

506   ENM concentrations are much more dilute than in the system studied here.

507   The difference between the measurements in synthetic and natural leachates points to another advantage of using

508   NTA to study the behavior of ENM in these solutions which is to differentiate between homo- and

509   heteroagglomeration. In solutions with only ENM as particles (i.e. in the DI H_2O or synthetic landfill leachate

510   samples), homoagglomeration is the only possibility when particles are unstable and they may subsequently

511   agglomerate and settle from solution. Conversely, in the solutions that contained additional particulate matter (i.e.

512   the natural particles and DOC in the natural leachate), the possibility exists for ENM to aggregate with other

513   materials (i.e. heteroagglomeration).

514   Despite having a lower maximum resolution of 10-30 nm and requiring a relatively high particle concentration (10^5 -

515   10^{10} particles/mL[28]), this technique i still useful to estimate the stability of particles in various solutions. Indeed,

516   when the number of particles studied in this manuscript is transformed to a mass based concentration (equating to

517   approximately 150 – 800 µg/L), the lower end of this concentration range is within an acceptable level to study

518   particle behavior at environmentally relevant concentrations, or is at least on par with other techniques which aer

519   commonly used and accepted as suitable for studying nanomaterial behavior at environmentally relevant

520   concentrations. The aim of this work was not to specifically study the dynamic range of the instrument (although the

521   upper particle number was determined), and so with additional method development it may be possible to determine

522   particle behavior at even lower concentrations than studied here. However, the technique does not provide details of

523   morphology and particle motion is recorded in two dimensions not three. The latter pitfall often leads to some tracks

524   being associated with a smaller degree of motion and consequently sized (incorrectly) as larger particles.[29]

525   Nevertheless, the ability to track agglomeration in real time in the native solution is a benefit of NTA that is not

526   readily duplicated by other nanometrology techniques.

527

528   *4.2 Size vs. mass-based evaluation in aqueous systems*

529   Many experiments that focus on ENM stability, for example with DLS as the main ENM characterization technique,

530   simply measure average particle size and estimate total concentration of particles in suspension over time. Often,

531   based on these metrics, one comes to the conclusion that the primary particle size increases (through agglomeration)

532   after being spiked into a solution and then when the concentration subsequently decreases, the researcher presumes

533   the particles sediment out of suspension. However, with the additional information generated by the NTA analysis,

534   transformation of the particle size distribution and particle number measured to mass of analyte shows that there are

535   often more complicated metrics at play. This is exemplified by our case study on the stability of ENM in synthetic

536   and natural landfill leachate solutions. When distributing the number of particles measured over the measured size

537   distribution to determine the mass of particles in solution, the mischaracterization of ENM size can grossly

538   overestimate the mass of Au in the system. Since the size of individual particles is independently tracked by the

539   NTA, the number of particles analyzed can be spread across the particle size distribution and subsequently be

540   converted to mass.[30] The mean obtained and reported from the NTA instrument is a number weighted average.

541   However, from the (raw) distribution obtained from the NTA output; volume, mass and intensity weighted means

542   (and histograms) can be calculated for each measurement recorded. When converting the size-based distribution to a

543   mass-based distribution, it becomes starkly evident that the presence of even a low number of large aggregates can

544   represent a significant proportion of the total mass in the sample.

545   Reporting both size and mass based metrics is common when dealing with other particulate matter, for example in

546   air.[31,32] Number- and mass-based analytical techniques are used and the results are routinely transformed from one

547   metric into another. This is not yet the case in water but now the NTA can give us the additional information that is

548   necessary in order to report results in both ways.

549   **5. Implications**

550   Beyond the finite results of our case study on the stability of ENM in landfill leachates, our goal was to further

551   investigate the advantages of using the NTA to study ENM in complex matrices. To that extent, there are several

552   facets of the technique that are specifically (and sometimes uniquely) beneficial to detect and size ENM, along with

553   characterizing their behavior in environmental media. Firstly, the ability to discretely measure ENM on top of the

554   natural particle background by taking advantage of the difference in the refractivity index of the particles in

555   particularly useful. While the NTA given particle concentration needs to be adjusted after making a calibration curve

556   of known values, a linear range can be obtained for each solution and the different concentrations of particles did not

557   change the measured particle size (distribution). Finally, by using the two metrics directly obtained from the NTA,

558 the particle size distribution and the particle concentration, one can calculate the mass of analyte in solution that can

559 provide an additional dynamic to understand the stability of particles in solution. Given the myriad of

560 nanometrology techniques that are continually being developed and improved in recent years, the options for

561 measurement and characterization of ENM are numerous. The benefit of measuring ENM directly in the native

562 solution with the additional advantage of discerning ENM from natural particles suggest that NTA is a useful tool

563 for measuring ENM in a variety of complex matrices.

564

565

566 **Acknowledgements**

570

571 **Funding Source**

574

575 **Supporting Information**

576 Au nanoparticle size distribution measurements, natural and synthetic leachate water chemistry analysis, median size

577 of particles measured by NTA at each time point (table and figure), measured particle number concentration in

578 solutions without adjustment based on calibration curve.

579

580

581

582

583

584

585

586

587

588

589

590

591

592

593

594

595

596

597

598

599

600

601

602
603
604
605
606
607
608
609
610

611   **References**
612   1.   Lowry, G. V.; Gregory, K. B.; Apte, S. C.; Lead, J. R., Transformations of Nanomaterials
613   in the Environment. *Environmental Science & Technology* **2012,** *46*, (13), 6893-6899.
614   2.   Mitrano, D. M.; Nowack, B., The need for a life-cycle based aging paradigm for
615   nanomaterials: Importance of real-world test systems to identify realistic particle
616   transformations. *Nanotechnology* **2017,** *28*, (7), 072001.
617   3.   Montaño, M. D.; Olesik, J. W.; Barber, A. G.; Challis, K.; Ranville, J. F., Single Particle
618   ICP-MS: Advances toward routine analysis of nanomaterials. *Analytical and Bioanalytical*
619   *Chemistry* **2016,** *408*, (19), 5053-5074.
620   4.   Laborda, F.; Bolea, E.; Cepriá, G.; Gómez, M. T.; Jiménez, M. S.; Pérez-Arantegui, J.;
621   Castillo, J. R., Detection, characterization and quantification of inorganic engineered
622   nanomaterials: A review of techniques and methodological approaches for the analysis of
623   complex samples. *Analytica chimica acta* **2016,** *904*, 10-32.
624   5.   Kim, H.-A.; Lee, B.-T.; Na, S.-Y.; Kim, K.-W.; Ranville, J. F.; Kim, S.-O.; Jo, E.; Eom, I.-C.,
625   Characterization of silver nanoparticle aggregates using single particle-inductively coupled
626   plasma-mass spectrometry (spICP-MS). *Chemosphere* **2017,** *171*, 468-475.
627   6.   Mitrano, D. M.; Arroyo Rojas Dasilva, Y.; Nowack, B., Effect of Variations of Washing
628   Solution Chemistry on Nanomaterial Physicochemical Changes in the Laundry Cycle.
629   *Environmental Science & Technology* **2015,** *49*, (16), 9665-9673.
630   7.   Prasad, A.; Lead, J.; Baalousha, M., An electron microscopy based method for the
631   detection and quantification of nanomaterial number concentration in environmentally
632   relevant media. *Science of the Total Environment* **2015,** *537*, 479-486.
633   8.   Dubascoux, S.; Hecho, I.; Hassellov, M.; Kammer, F.; Gautier, M.; Lespes, G., Field-flow
634   fractionation and inductively coupled plasma mass spectrometer coupling: History,
635   development and applications. *Journal of Analytical Atomic Spectrometry* **2010,** *25*, (5),
636   613-623.
637   9.   Loeschner, K.; Navratilova, J.; Legros, S.; Wagner, S.; Grombe, R.; Snell, J.; von der
638   Kammer, F.; Larsen, E. H., Optimization and evaluation of asymmetric flow field-flow
639   fractionation of silver nanoparticles. *Journal of Chromatography A* **2013,** *1272*, 116-125.
640   10.   Wagner, S.; Legros, S.; Löschner, K.; Liu, J.; Navratilova, J.; Grombe, R.; Linsinger, T.;
641   Larsen, E.; Von Der Kammer, F.; Hofmann, T., First steps towards a generic sample
642   preparation scheme for inorganic engineered nanoparticles in a complex matrix for
643   detection, characterization, and quantification by asymmetric flow-field flow fractionation
644   coupled to multi-angle light scattering and ICP-MS. *Journal of Analytical Atomic*
645   *Spectrometry* **2015,** *30*, (6), 1286-1296.
646   11.   Hassellöv, M.; Kaegi, R., *Analysis and characterization of manufactured nanoparticles*
647   *in aquatic environments*. John Wiley & Sons, Inc.: United Kingdom: 2009.
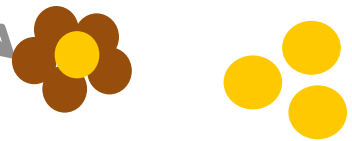
648   12.   Gillespie, C.; Halling, P.; Edwards, D., Monitoring of particle growth at a low
649 concentration of a poorly water soluble drug using the NanoSight LM20. *Colloids and*
650 *Surfaces A: Physicochemical and Engineering Aspects* **2011,** *384*, (1), 233-239.
651   13.   Whitepaper, M., Nanoscale Material Characterization: a Review on the use of
652 Nanoparticle Tracking Analysis (NTA). **2015**.
653   14.   Sanchís, J.; Bosch-Orea, C.; Farré, M.; Barceló, D., Nanoparticle tracking analysis
654 characterisation and parts-per-quadrillion determination of fullerenes in river samples
655 from Barcelona catchment area. *Analytical and bioanalytical chemistry* **2015,** *407*, (15),
656 4261-4275.
657   15.   Bartczak, D.; Vincent, P.; Goenaga-Infante, H., Determination of size-and number-
658 based concentration of silica nanoparticles in a complex biological matrix by online
659 techniques. *Analytical chemistry* **2015,** *87*, (11), 5482-5485.
660   16.   Gallego-Urrea, J. A.; Tuoriniemi, J.; Hassellöv, M., Applications of particle-tracking
661 analysis to the determination of size distributions and concentrations of nanoparticles in
662 environmental, biological and food samples. *TrAC Trends in Analytical Chemistry* **2011,** *30*,
663 (3), 473-483.
664   17.   Mueller, N.; Nowack, B., Exposure modeling of engineered nanoparticles in the
665 environment. *Environmental Science and Technology* **2008,** *42*, (12), 4447-4453.
666   18.   Gottschalk, F.; Scholz, R.; Nowack, B., Probabilistic material flow modeling for
667 assessing the environmental exposure to compounds: Methodology and an application to
668 engineered nano-TiO2 particles. *Environmental Modelling & Software* **2010,** *25*, (3), 320-
669 332.
670   19.   Sun, T. Y.; Gottschalk, F.; Hungerbühler, K.; Nowack, B., Comprehensive probabilistic
671 modelling of environmental emissions of engineered nanomaterials. *Environmental*
672 *Pollution* **2014,** *185*, 69-76.
673   20.   Keller, A. A.; McFerran, S.; Lazareva, A.; Suh, S., Global life cycle releases of
674 engineered nanomaterials. *Journal of Nanoparticle Research* **2013,** *15*, (6), 1-17.
675   21.   Mitrano, D. M.; Motellier, S.; Clavaguera, S.; Nowack, B., Review of nanomaterial
676 aging and transformations through the life cycle of nano-enhanced products. *Environment*
677 *international* **2015,** *77*, 132-147.
678   22.   Thio, B.; Montes, M. O.; Mahmoud, M.; Lee, D.; Zhou, D.; Keller, A., Mobility of Capped
679 Silver Nanoparticles under Environmentally Relevant Conditions. *Environ Sci Technol* **2012,**
680 *46*, (13), 6985-6991.
681   23.   Kiser, M.; Ryu, H.; Jang, H.; Hristovski, K.; Westerhoff, P., Biosorption of
682 nanoparticles to heterotrophic wastewater biomass. *Water Research* **2010,** *44*, 4105-4114.
683   24.   Limbach, L. K.; Bereiter, R.; MuÃàller, E.; Krebs, R.; GaÃàlli, R.; Stark, W. J., Removal
684 of oxide nanoparticles in a model wastewater treatment plant: Influence of agglomeration
685 and surfactants on clearing efficiency. *Environmental science & technology* **2008,** *42*, (15),
686 5828-5833.
687   25.   Mitrano, D. M.; Mehrabi, K.; Dasilva, Y. A. R.; Nowack, B., Mobility of metallic
688 (nano)particles in leachates from landfills containing waste incineration residues.
689 *Environmental Science: Nano* **2017,** *4*, (2), 480-492.
690   26.   Mitrano, D. M.; Ranville, J.; Bednar, A.; Kazor, K.; Hering, A. S.; Higgins, C., Tracking
691 dissolution of silver nanoparticles at environmentally relevant concentrations in
692 laboratory, natural and processed waters using single particle ICP-MS (spICP-MS).
693 *Environmental Science: Nano* **2014,** *1*, (3), 248-259.

694   27.   Van Der Pol, E.; Coumans, F. A.; Sturk, A.; Nieuwland, R.; van Leeuwen, T. G.,
695   Refractive index determination of nanoparticles in suspension using nanoparticle tracking
696   analysis. *Nano letters* **2014,** *14*, (11), 6195-6201.
697   28.   Malloy, A.; Carr, B., Nanoparticle tracking analysis–the Halo™ system. *Particle &*
698   *Particle Systems Characterization* **2006,** *23*, (2), 197-204.
699   29.   Saveyn, H.; De Baets, B.; Thas, O.; Hole, P.; Smith, J.; Van Der Meeren, P., Accurate
700   particle size distribution determination by nanoparticle tracking analysis based on 2-D
701   Brownian dynamics simulation. *Journal of colloid and interface science* **2010,** *352*, (2), 593-
702   600.
703   30.   La Rocca, A.; Di Liberto, G.; Shayler, P.; Parmenter, C.; Fay, M., Application of
704   nanoparticle tracking analysis platform for the measurement of soot-in-oil agglomerates
705   from automotive engines. *Tribology International* **2014,** *70*, 142-147.
706   31.   Harrison, R. M.; Shi, J. P.; Xi, S.; Khan, A.; Mark, D.; Kinnersley, R.; Yin, J., Measurement
707   of number, mass and size distribution of particles in the atmosphere. *Philosophical*
708   *transactions of the royal society of London A: mathematical, physical and engineering*
709   *sciences* **2000,** *358*, (1775), 2567-2580.
710   32.   Anastasio, C.; Martin, S. T., Atmospheric nanoparticles. *Reviews in Mineralogy and*
711   *Geochemistry* **2001,** *44*, (1), 293-349.

712

NanoSight
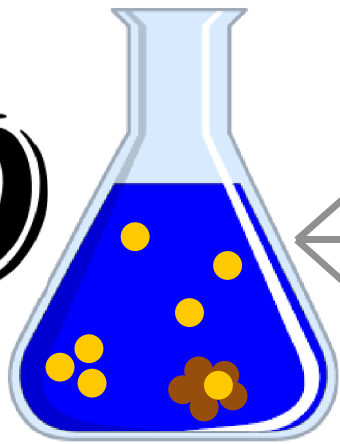
Landfill Leachate

Particle size and number

Analyte mass and particle stability

Homo- vs. Heteroaggregation